

AN RF POWERED, WIRELESS TEMPERATURE SENSOR IN QUARTER MICRON CMOS

Fatih Kocer, Paul M. Walsh, and Michael P. Flynn

Wireless Integrated Microsystems Engineering Research Center (WIMS-ERC)
University of Michigan, Ann Arbor, MI 48109

ABSTRACT

We present a wireless CMOS temperature sensor that gathers power through RF power telemetry, and transmits data wirelessly at 2.3GHz to a base station. Power is gathered by a low threshold voltage rectifier-multiplier circuit decreasing the minimum incident peak signal amplitude required at the receiving port compared to the state of the art power telemetry systems. A low power integrated LC voltage controlled oscillator (VCO) lies at the heart of the system. The oscillation frequency of the VCO is modulated by change in the ambient temperature, and is transmitted via an integrated power amplifier. The measured phase noise of the oscillator is -101dBc/Hz (@1Mhz offset) while consuming $400\mu\text{A}$, achieving a figure of merit of 171dBc/Hz . A linear temperature sensitivity of $126\text{ppm}/^\circ\text{C}$ is achieved with a total sensor current consumption of 1.1mA .

1. INTRODUCTION

Wired CMOS temperature sensors have been widely used for more than three decades for various applications [1,2]. Wireless, batteryless operation will significantly increase the utility of these devices.

Wireless telemetry of power and data has been demonstrated successfully in implanted biomedical systems [3]. The lifetime of RFID tags is increased with the removal of the battery, and power is generated via inductive coupling with the base station [4].

A block diagram of a conventional active telemetry system is shown in Fig. 1. The incident RF power is inductively coupled to the receiver, rectified and stored to power the system. The clock is extracted from the incident RF signal by a Schmitt trigger circuit. Data is then sent to the power amplifier to be transmitted. The distance between the base station and the receiver, however, must be very small (usually in millimeters), so that efficient coupling is achieved between the base station and the receiver. This ensures that the voltage swing at the receiving port is large enough to be rectified and used as a voltage supply (usually around 3V-5V).

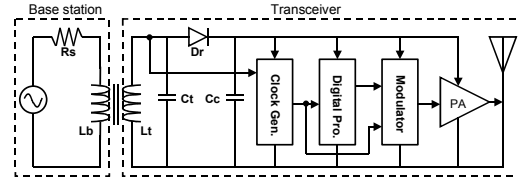


Fig. 1. Block diagram of an active telemetry system

We describe new techniques that generate the supply voltage from a weaker received signal. In order to decrease the overall power consumption, we employ a fully integrated local oscillator rather than a clock extraction circuit. A high operation frequency (2.3GHz) is selected, so that miniature high gain antennas can be used decreasing the overall system size.

2. TRANSCEIVER ARCHITECTURE

A block diagram of the proposed transceiver architecture is given in Fig. 2. An RF-DC converter generates a DC voltage much higher than the zero to peak amplitude of the incident RF signal and stores it on a large storage capacitor. This voltage is then used as the supply voltage for the whole system. The converter incorporates a low threshold rectifier and multiplier circuit, which works for weaker incident signal.

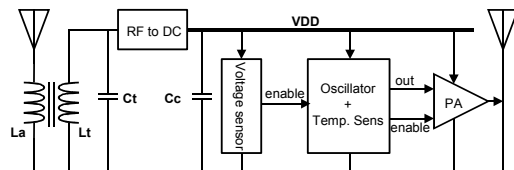


Fig. 2. Block diagram of the proposed transceiver

The control voltage of a voltage-controlled oscillator (VCO) changes by the ambient temperature changes. In this way, the temperature data is converted to a shift in the oscillation frequency. The VCO output is sent to a pseudo-differential class AB power amplifier (PA) to be transmitted wirelessly. A bias network generates the bias current for all the circuit blocks, and also provides a temperature dependent voltage output to be used as the control voltage of the VCO.

A voltage sensor enables the system whenever the voltage on the storage capacitor is larger than 2.5V, and puts it into a stand-by mode when the voltage drops below 1.5V. In standby mode, the whole system consumes an average of 5 μ A, allowing the capacitor to recharge.

Since the power stored on the charging capacitor is used as the supply voltage of the rest of the circuit blocks, the capacitor is discharging during the active operation. Therefore, overall power consumption determines the length of this active time. We designed the circuit blocks to have low power consumption while active, and very low standby current while powered down. On the other hand, since the system has to operate under a varying supply voltage from 1.5V to 2.5V, we use circuit architectures with high supply rejection and cascode devices wherever possible. We now discuss the sub-blocks.

2.1. RF to DC Converter

A Dickson [5] multiplier circuit with multiple stages is used to generate a DC voltage higher than the peak signal amplitude at the receiving port. A block diagram and the schematic details of one stage are given in Fig. 3. We chose a Dickson multiplier over a clocked voltage doubler circuit, since latter needs a fast clock and consumes clock power during switching and due to switching losses.

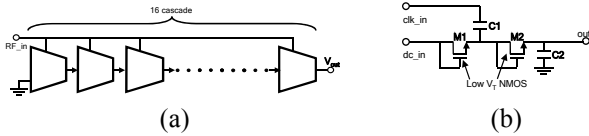


Fig. 3. (a) Block diagram of the multiplier, and (b) the schematic detail of one of the stages.

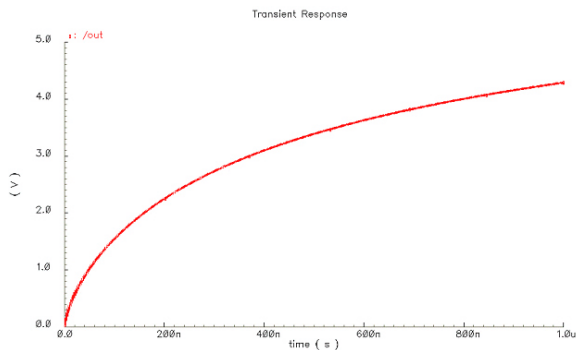


Fig. 4. Simulation results of the RF-DC converter

We use zero V_T transistors as diodes in order to minimize voltage drop. Metal-insulator-metal (MiM) capacitors are used to decrease the overall area of the multiplier array. As can be seen from the simulation results in Fig.4 an RF peak voltage of 300mV at the input is enough to generate a 2.5V_{DC} at the output.

2.2. VCO, Temperature Sensor, and the PA

We employ a fully integrated LC VCO as the local oscillator and the temperature sensor of the system. The schematic of the LC oscillator and the bias network is given in Fig. 5.

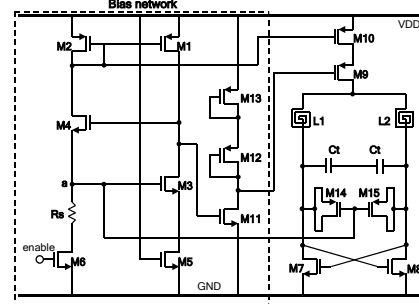


Fig. 5. Schematics of LC oscillator and bias network

A PTAT voltage source sets the control voltage on MOS varactors M14 and M15, causing the oscillator frequency to vary with temperature. Since the voltage of the node **a** on the bias network is equal to the threshold voltage V_T of M3, it is independent of the supply variations but affected by the ambient temperature changes. This makes it a perfect candidate as the PTAT voltage source. The control inputs of varactors are connected to the node **a**, so that any change in temperature changes the control voltage on the varactors. This in turn modulates the output frequency of the oscillator.

We use an NMOS only cross-coupled architecture (M7-M8) rather than a CMOS cross-coupled architecture [6] to have larger headroom and reduce the minimum supply voltage.

In order to achieve low power consumption, the oscillator is operated in current limited mode [7]. The oscillation criterion for an LC oscillator is given as:

$$R_p > \frac{1}{g_m} \quad (1)$$

where R_p is the effective parallel resistance of the tank, and g_m is the negative transconductance generated by the cross-coupled pair. In order to achieve the smallest power consumption, R_p should be increased as large as possible so that g_m can be minimized. The parallel resistance value R_p is given as:

$$R_p = \frac{L_s}{C_t \times R_s} \quad (2)$$

where L_s is the series inductance, R_s is the series resistance, and C_t is the tank capacitance. We use an inductance of 8.5nH and a tank capacitance of 560fF to achieve the 2.3GHz oscillation with a quiescent current of 400 μ A.

The long channel length transistor M9 increases the supply rejection of the oscillator, since it isolates the LC tank from the VDD line. The bias for M9 is generated by the high threshold transistor string M11-M12-M13.

Transistor M6 on the bias network works as a switch to turn the bias circuit on and in turn, enable the VCO. The enable signal is supplied by the voltage sensor and is a linear function of VDD, as will be discussed in the next section. Since it is a function of the supply voltage, the channel resistance of M6 changes with the supply voltage change. The gate of M5 is connected to VDD to compensate for this change. The current generated in the bias network is determined by the threshold voltage, V_T , of M3 and the resistance of R_s . We use a medium threshold transistor M3 to generate a low quiescent current while keeping the design compact with smaller resistance value.

We use a fully integrated pseudo-differential class AB power amplifier for this prototype device as shown in Fig 6a. The inductors are 12nH, with a simulated quality factor Q of 5. A cascode topology provides unconditional stability by isolating the gates of M1 and M2 from the output tank preventing self-resonance [8]. Moreover cascading increases output resistance. The quiescent current of the PA is 0.7mA. Since the DC bias of the PA is supplied by the VCO, the VCO enable signal also enables the PA, limiting the power consumption.

2.2. Voltage Sensor

A very low quiescent current ($<1\mu A$) Schmitt trigger, as shown in Fig. 6b, senses the voltage stored on the capacitor and creates an enable signal to turn on the temperature sensor and the power amplifier. It turns the system on via transistor M6 of Fig .4, whenever the voltage level on the capacitor is larger than 2.5V and turns it off when it drops below 1.5V.

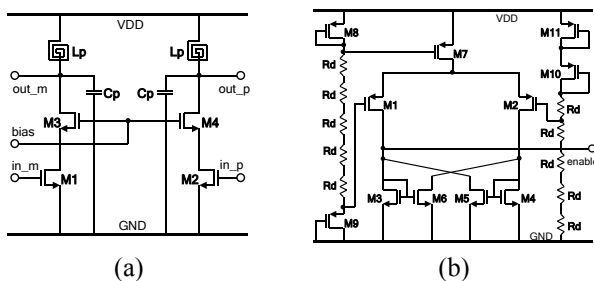


Fig. 6. Schematic of the (a) PA, and (b) voltage sensor

Large valued resistors are used in the resistor ladder to decrease the static power dissipation. We use N-Well resistors, which provide the largest on-chip resistance values, to keep the circuit compact. Two high threshold diode connected transistors are used to turn-off the resistor ladder below 1.5V to further decrease power dissipation.

2. TEST RESULTS AND DISCUSSION

The device was fabricated in the TSMC 0.25 μm mixed-mode process. The process incorporates medium and zero threshold transistors and thick top metal. The design has electrostatic discharge (ESD) protection on all pads. The active device area is 1.2mm², without the charging capacitors. A microphotograph of the circuit is given in Fig. 7a. The die is packaged into a 52 pin ceramic LCC package. An impedance controlled PCB, which is shown in Fig. 7b, is designed to decrease the reflections and losses during the high frequency tests. The device is soldered directly on to the board to decrease the parasitic effects.

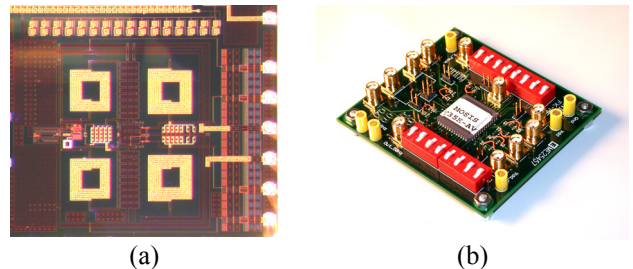


Fig. 7. Picture of (a) die, (b) test PCB

We used a humidity controlled temperature chamber to perform the temperature sweep tests. Fig. 8 shows the temperature sweep test results of the prototype chip. A temperature sensitivity of 126ppm/ $^{\circ}C$ is achieved over a range from $-40^{\circ}C$ to $40^{\circ}C$ with a coefficient of determination of 0.983.

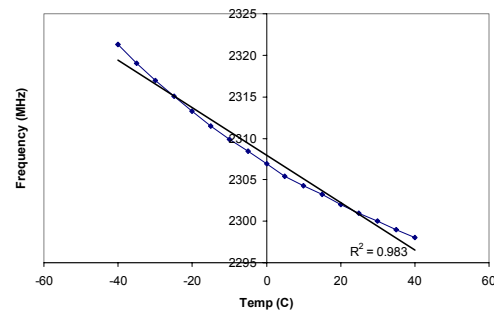


Fig. 8. Temperature sweep results

The phase noise of the system is measured as $-101\text{dBc}/\text{Hz}$ at 1Mhz offset at room temperature, as shown in Fig. 9. This corresponds to a figure of merit (FOM) [9] of $171\text{dBc}/\text{Hz}$ using the formula:

$$FOM = -SSB - 20\log\left(\frac{\Delta f}{f}\right) - 10\log\left(\frac{P_{dis}}{1mW}\right) \quad (3)$$

where, SSB is the phase noise at the offset frequency Δf , f is the carrier frequency, and P_{dis} is the power dissipation.

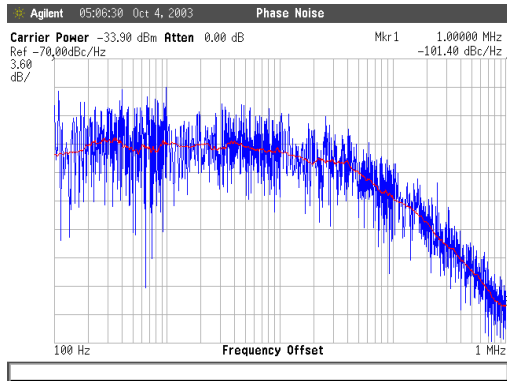


Fig. 9. Phase noise measurement

The system shows good rejection to supply voltage changes, with a change of 70kHz over a supply sweep of 1V. This corresponds to a supply sensitivity of 28ppm/V.

In order to test the functionality of the voltage sensor, we sweep the voltage from 0V to 2.5V, and back to 0V and measure the total current passing through the system. As can be seen from Fig.10, the hysteresis curve clearly indicates the system operation.

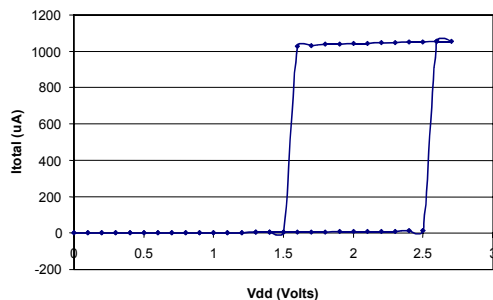


Fig. 10. Voltage sensor operation results

3. CONCLUSION

We present a wireless temperature sensor working at 2.3GHz. It gathers power from an incident RF signal. A novel way of RF to DC conversion is used to reduce the signal strength needed at the receiving port. This enables the distance between the base and the receiver to be increased. A low power LC VCO is used as the temperature sensor. The system has a temperature sensitivity of 126ppm/°C and a measured phase noise of -101dBc/Hz at 1MHz offset, which corresponds to a FOM of 171dBc/Hz.

The device stays in a stand-by mode with very low power consumption, until the RF-DC converter stores enough energy to operate the transceiver. When enabled it consumes a total of 1.1mA transmitting the temperature information at 2.3GHz.

The device is fabricated in TSMC 0.25 μm mixed-mode process. The total active area is smaller than

1.2mm² (excluding the charging caps). A summary of the overall device specifications is given in Table 1.

Table 1. Summary of the system

Technology	TSMC 0.25 μm , 1.2mm ² active area	
Carrier frequency	2.3GHz	
Temperature sens.	126ppm/°C	
Supply sens.	28ppm/V	
Power Consumption	Stand-by	Active
	5 μA	1.1mA
Phase Noise	-101dBc/Hz (@1MHz offset)	
FOM	171dBc/Hz	

4. ACKNOWLEDGMENTS

This work was supported by the WIMS-ERC, Engineering Research Centers program of the NSF under Award Number EEC-9986866. The authors acknowledge the assistance of Ivan Bogue, and Robert Gordenker. The IC was fabricated by MOSIS through the MEP program.

5. REFERENCES

- [1] G. C. M. Meijer, "Thermal Sensors Based on Transistors," *Sensors and Actuators*, vol. 10, pp. 103-125, 1986.
- [2] Szekely *et al*, "CMOS temperature sensors and built-in test circuitry for thermal testing of ICs," *Sensors and Actuators, A: Physical*, vol. 71, pp. 10-18, 1998.
- [3] Q. Huang and M. Oberle, "0.5-mW passive telemetry IC for biomedical applications," *IEEE Journal of Solid-State Circuits*, vol. 33, pp. 937-946, 1998.S.
- [4] Masui *et al*, "13.56MHz CMOS RF identification transponder integrated circuit with a dedicated CPU," *Digest of Technical Papers IEEE International Solid State Circuits Conference*, vol. 1999, pp. 162-163, 1999.
- [5] J. F. Dickson, "On-Chip High-Voltage Generation in Mnos Integrated Circuits Using an Improved Voltage Multiplier Technique," *IEEE J Solid State Circuits*, pp. 374-378, 1976.
- [6] A. Hajimiri and T. H. Lee, "Design issues in CMOS differential LC oscillators," *IEEE Journal of Solid-State Circuits*, vol. 34, pp. 717-724, 1999.
- [7] D. Ham and A. Hajimiri, "Concepts and methods in optimization of integrated LC VCOs," *IEEE Journal of Solid State Circuits*, vol. 36, pp. 896-909, 2001.
- [8] S. T. Cripps, *RF power amplifiers for wireless communications Amplifiers*, Artech House, Boston, 1999.
- [9] M. Tiebout, "Low-power low-phase-noise differentially tuned quadrature VCO design in standard CMOS," *IEEE Journal of Solid State Circuits*, vol. 36, pp. 1018-1024, 2001.